



## Cell surface localised Hsp70 is a cancer specific regulator of clathrin-independent endocytosis



Benedikt Nimmervoll<sup>a</sup>, Lilia A. Chtcheglova<sup>a,b</sup>, Kata Juhasz<sup>a</sup>, Nunilo Cremades<sup>c</sup>, Francesco A. Aprile<sup>c</sup>, Alois Sonnleitner<sup>a</sup>, Peter Hinterdorfer<sup>a,b</sup>, Laszlo Vigh<sup>d</sup>, Johannes Preiner<sup>a</sup>, Zsolt Balogi<sup>a,e,\*</sup>

<sup>a</sup> Center for Advanced Bioanalysis GmbH, Linz, Austria

<sup>b</sup> Institute for Biophysics, Johannes Kepler University, Linz, Austria

<sup>c</sup> Department of Chemistry, University of Cambridge, Cambridge, United Kingdom

<sup>d</sup> Institute of Biochemistry, Biological Research Centre, Hungarian Academy of Sciences, Szeged, Hungary

<sup>e</sup> Institute of Experimental Medicine, Hungarian Academy of Sciences, Budapest, Hungary

### ARTICLE INFO

#### Article history:

Received 3 May 2015

Revised 1 July 2015

Accepted 19 July 2015

Available online 6 August 2015

Edited by Lukas Huber

#### Keywords:

Hsp70

Endocytosis

Cancer

Membrane

Clustering

### ABSTRACT

The stress inducible heat shock protein 70 (Hsp70) is present specifically on the tumour cell surface yet without a pro-tumour function revealed. We show here that cell surface localised Hsp70 (sHsp70) supports clathrin-independent endocytosis (CIE) in melanoma models. Remarkably, ability of Hsp70 to cluster on lipid rafts *in vitro* correlated with larger nano-domain sizes of sHsp70 in high sHsp70 expressing cell membranes. Interfering with Hsp70 oligomerisation impaired sHsp70-mediated facilitation of endocytosis. Altogether our findings suggest that a sub-fraction of sHsp70 co-localising with lipid rafts enhances CIE through oligomerisation and clustering. Targeting or utilising this tumour specific mechanism may represent an additional benefit for anti-cancer therapy.

© 2015 Federation of European Biochemical Societies. Published by Elsevier B.V. All rights reserved.

### 1. Introduction

Members of the Hsp70 family assist in the folding of nascent or misfolded proteins with an important role in cellular protein homeostasis [1]. Frequently upregulated in tumour cells [2], inducible Hsp70 (HSPA1A) exerts cytoprotective and anti-apoptotic functions [3]. Unlike the constitutive homologue Hsc70, Hsp70 is also known to be present at the extracellular leaflet of the plasma membrane (surface Hsp70, sHsp70) of most tumour cells but not that of the corresponding normal cells [4]. sHsp70 has been identified as a recognition feature for the immune system [5]. At the same time, the concentration of sHsp70 has been shown to correlate with metastatic potential of B16 mouse melanoma cells [6]. As surface localisation of Hsp70 is dependent on cholesterol content of the membrane, sHsp70 is likely associated with “lipid rafts” [7].

Given that Hsp70 is frequently upregulated in tumour cells, where it is specifically present on the tumour cell surface, and that derailed endocytosis is a feature of cancer [8], we hypothesized that sHsp70 may have a general impact on the endocytic process. We previously showed that overexpression of Hsp70 in B16 mouse melanoma cells gave rise to the concentration of sHsp70 [9]. Here we show for the first time, using the B16 model and human A375 melanoma cells, that high levels of Hsp70 facilitate CIE even at unstressed conditions. We further reveal that a sub-fraction of sHsp70 localised in lipid rafts facilitates CIE through its oligomerisation and clustering in the plasma membrane.

### 2. Materials and methods

Inducible cell lines of B16-F10 and A375 (ATCC, Manassas, VA, USA) were generated by co-transfection of cells with pcDNA.6/TR and with empty pcDNA.4/TO or pcDNA.4/TO-mHSP70 or pcDNA.4/TO-mHsp70-E3. Stable clones were selected by media containing Zeocin (Life Technologies) and Blasticidin (InvivoGen, San Diego, CA, USA). B16-F10 cells were cultured in RPMI medium (Life Technologies) supplemented with 10% FCS (Sigma-Aldrich, St. Louis, MO, USA), 2 mM L-glutamine (Life Technologies), A375 cells

**Author contributions:** ZB, BN, JP conceived the study; BN, LAC, JP, ZB, KJ performed the experiments; BN, LAC, JP, ZB, LV analysed the data; AS, PH, ZB, NC, FAA provided reagents and tools; all authors discussed the results and wrote the paper.

\* Corresponding author at: Institute of Experimental Medicine, Hungarian Academy of Sciences, Budapest, Hungary. Fax: +36 1 210 9423.

E-mail addresses: [balogi.zsolt@koki.mta.hu](mailto:balogi.zsolt@koki.mta.hu), [zsolt.balogi@gmail.com](mailto:zsolt.balogi@gmail.com) (Z. Balogi).

in DMEM/F12 (+L-glutamine) (Life Technologies) with 10% FCS (Life Technologies). Hsp70 overexpression was induced by 2 µg/ml doxycycline for 16 h, referred to as “Hsp70”. Hsp70 expression levels were tested by Western blotting and flow cytometry. Experiments with fluorescent readout were performed in OptiMEM supplemented with 1% FCS (Sigma).

To determine endocytic pathway activities, cells were incubated for 5 min at 37 °C with 7.5 µM FM4-64 (Sigma) or 1.5 µM BODIPY-lactosylceramide (LacCer, Life Technologies) or 5 µg/ml transferrin-AlexaFluor488 (Tf, Life Technologies). Following the incubation, cells were washed twice in ice-cold medium. LacCer was back-exchanged in 6 × 10 min washing steps with 5% defatted BSA (Sigma) in ice-cold OptiMEM. Samples were analysed by flow cytometry (BD FACS Aria, Becton Dickinson, Franklin Lakes, NJ, USA) with an excitation at 488 nm or 633 nm and detection at 530/30 nm or at 695/40 nm for Tf and LacCer or for FM4-64, respectively. Debris and cells with damaged membranes were gated by FSC vs. SSC plotting and propidium-iodide exclusion (5 µg/ml, Sigma). The extracellular Tf signal was quenched by 0.1% trypan blue (Sigma).

For the identification of sHsp70 endocytosis pathways, induced cells were pre-incubated for 30 min with 10 µg/ml chlorpromazine (Sigma) or 2 mM amantadine (Sigma) for inhibition of CDE or with 50 µg/ml nystatin (Millipore) or 1 mM methyl-β-cyclodextrin (MβCD, Sigma) for inhibition of CIE. Then, Alexa488 labelled (Life Technologies) cmHsp70.1 antibody (multimmune, München, Germany) or appropriate isotype control (Sigma) was added (1 µg/50 µl) at 37 °C for 30 min for endocytosis. Cells were washed in ice-cold medium and the intracellular fluorescence was determined by flow cytometry in the 530/30 nm channel. Live cell gating and quenching of extracellular signal were performed as described above.

To inhibit endocytosis by sHsp70 immobilisation, 96-well plates were coated with cmHsp70.1 or isotype control (2 mg/ml) in a 0.05 M sodium carbonate buffer (pH 9.6), at 4 °C overnight. 2 µm beads coated with goat anti-mouse IgG (chemicell, Berlin, Germany) were loaded with cmHsp70.1 or isotype control (2 µg/mg bead). 150 µg of beads were distributed per well and incubated for 1 h at 37 °C. To determine the endocytic activity, cells were incubated in 100 µl of ice-cold medium containing 7.5 µM FM4-64 (Sigma) for 5 min and endocytosis was initiated by releasing the cold block at 37 °C for another 5 min. Following extensive washing, FM4-64 was excited at 500/9 nm and the fluorescence signal was measured at 730/20 nm in a plate reader (Tecan Infinite Pro, Tecan, Maennedorf, Switzerland). Cell-free wells served as background control.

To study endocytosis in the presence of Hsp70 oligomerisation inhibitors, cells plated onto 96-well plates were induced to overexpress Hsp70 for 12 h. Next, cells were incubated with Hsp70 peptide fragments generated as described in Aprile et al. [10] or with BSA (10–1000 nM) at 37 °C for 16 h. Then endocytosis of FM4-64 was measured as described above with the temperature block performed at room temperature (20 °C).

The Hsp70 surface distribution on cell surfaces was studied under physiological conditions by simultaneous topography and recognition imaging (TREC). TREC is based on atomic force microscopy in combination with a recognition molecule on the tip of the cantilever, which enables simultaneous sensing of topography and recognition of proteins with nanometre accuracy. TREC was performed on a commercially available AFM set-up, a PicoPlus AFM 5500 (Agilent Technologies Inc., Chandler, AZ, USA) in magnetic AC (MAC) mode equipped with a PicoTREC box (Agilent Technologies Inc., Chandler, AZ, USA). Here the magnetically coated AFM tips (MACLevers, Type VII, Agilent Technologies Inc., AZ, USA) were functionalized with an antibody directed against surface Hsp70, isotype control, or the K4 peptide complementary for the

E3 tag on transgenic Hsp70. See [Supplementary material and methods](#) for full details.

For high-speed atomic force microscopy measurements 1 µg/ml recombinant Hsp70 was incubated on a freshly cleaved mica surface in PBS buffer for 5 min followed by several rinsing steps to remove unattached molecules from the liquid cell. Supported lipid bilayers in PBS buffer supplemented with 10 mM MgCl<sub>2</sub> were prepared from dioleoyl-phosphatidylcholine (PC)/octadecanoyl-sphingomyelin (SM)/cholesterol (65/25/10 molar ratio; Avanti Polar Lipids Inc., Alabaster, AL, USA) vesicles as described in [11].

Values in the text and graphs are presented as mean ± S.D. P-values are indicated in the graphs and were considered statistically significant when <0.05.

For a complete list of materials and methods used in this study please refer to the [Supplementary information](#).

### 3. Results and discussion

To determine whether Hsp70 expression levels generally have an impact on the endocytic activity in unstressed cells, we used stably transfected tetracycline-inducible systems for Hsp70 overexpression in mouse B16 and human A375 melanoma cells (Hsp70) [9]. Cells stably transfected with empty vector served as control (ctrl). We measured the activity of endocytic pathways through the uptake of the established fluorescent tracers FM4-64 for general endocytic activity, transferrin-AlexaFluor488 (Tf) for clathrin-dependent endocytosis (CDE) and BODIPY-lactosylceramide (LacCer) for clathrin-independent endocytosis (CIE) [12]. Upon Hsp70 overexpression in B16 and A375 cells, uptake of LacCer was significantly increased, while Tf uptake was slightly reduced (Fig. 1A). The latter observation was somewhat surprising, as previous reports on hepatoblastoma cells showed enhanced CDE, yet upon heat shock or pharmacological Hsp70 induction [13]. In fact, at stress conditions Hsp70 has been proposed to be able to substitute for Hsc70 in clathrin coat disassembly during CDE. In this current study, endocytosis has been measured at unstressed conditions, and a slight decrease in CDE may be attributed to excess of sHsp70 competing with Tf as a substrate of CDE. This explanation is supported by the fact that a large fraction of sHsp70 (60%) is endocytosed via CDE (Fig. 1B). Importantly, B16 cells with low basal level of Hsp70 displayed a considerable increase (+30.0%) in their general endocytosis levels, attributable to an increase in CIE. A smaller difference measured for A375 cells with high basal level of Hsp70 pointed to a saturating effect of overexpression (Fig. 1C). Given the higher response upon Hsp70 overexpression, B16 cells and the robust marker FM4-64 were used in further experiments.

As an attempt to specifically interfere with Hsp70-mediated endocytosis, we applied a specific antibody (cmHsp70.1) recognising the substrate-binding subdomain (SBSD) of sHsp70. Apparently, this treatment had no effect on endocytosis (Fig. 1D), indicating that substrate binding of Hsp70 may not be necessary for Hsp70-mediated endocytosis. Since the Hsp70-antibody adduct retains mobility of sHsp70 [9], we next targeted sHsp70 by anti-Hsp70 antibody (cmHsp70.1) immobilised on bead and well surfaces (see drawing in Fig. 1E). Importantly, this approach was specific to sHsp70 and revealed a sizeable facilitation of endocytosis by sHsp70 in Hsp70 overexpressing cells (44.5% and 18.3% inhibition with antibody-coated bead + well and bead surfaces, respectively). It is noted that no significant inhibition of endocytosis was detected for control, low Hsp70 expressing cells (data not shown). As soluble anti-Hsp70 antibody did not have any effect on FM4-64 uptake of Hsp70 overexpressing cells (Fig. 1D), we conclude that limiting Hsp70 mobility itself, and no other eventually allosteric effects induced by the antibody, reduced endocytic activity.

The finding that mobility of sHsp70 was required for its effect on endocytosis indicated that stimulation of endocytosis required

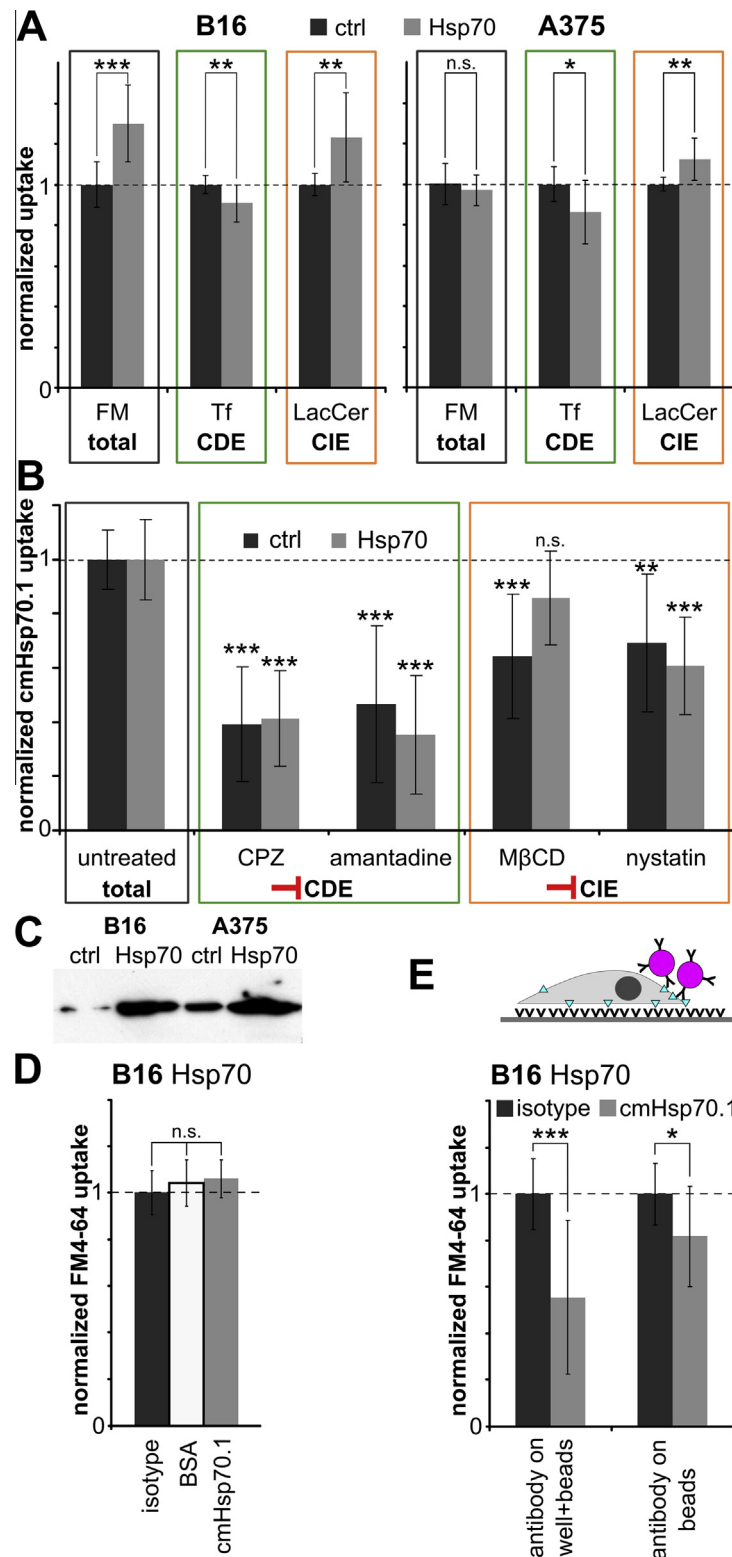


**Fig. 1.** Cell surface localised Hsp70 facilitates clathrin-independent endocytosis. (A) Activity of endocytosis pathways at different levels of intracellular Hsp70. Uptake of the fluorescent, pathway specific endocytosis tracers FM4-64 for total endocytosis, Alexa488-conjugated transferrin (Tf) for clathrin-dependent endocytosis and Bodipy-FL labelled lactosylceramide (LacCer) for clathrin-independent endocytosis was examined by flow cytometry in Hsp70 overexpressing mouse B16-F10 (B16) and human A375 melanoma cell lines (two-sided *t*-test, *P*-values indicated in the graph; *n* = 9–12; *N* = 3). (B) Endocytosis pathways utilised by Hsp70 in B16 cells. Endocytic pathways were specifically blocked with the clathrin-dependent endocytosis (CDE) inhibitors chlorpromazine (CPZ) and amantadine or with the clathrin-independent (CIE) endocytosis inhibitors methyl- $\beta$ -cyclodextrin (M $\beta$ CD) and nystatin. Endocytosis of Hsp70 was followed with Alexa488-conjugated cmHsp70.1 antibody and determined by flow cytometry. Indicated significance levels refer to the respective untreated condition. Hsp70 overexpression did not affect sHsp70 uptake routes (*P* = 0.829). (General linear model and subsequent Tukey's test; *n* = 8–15; *N* = 2–3). (C) Western blot analysis of Hsp70 expression levels in control (ctrl) and Hsp70 overexpressing cells. (D) FM4-64 uptake determined by flow cytometry in Hsp70 overexpressing B16 cells treated with anti-Hsp70 antibody (cmHsp70.1) or isotype control (one-way ANOVA; *n* = 11–12; *N* = 3). (E) FM4-64 uptake in Hsp70 overexpressing cells in the presence of anti-Hsp70 antibody coated beads and well surfaces immobilising sHsp70 was followed on a plate reader (one-sided *t*-test; *n* = 9–14; *N* = 3).



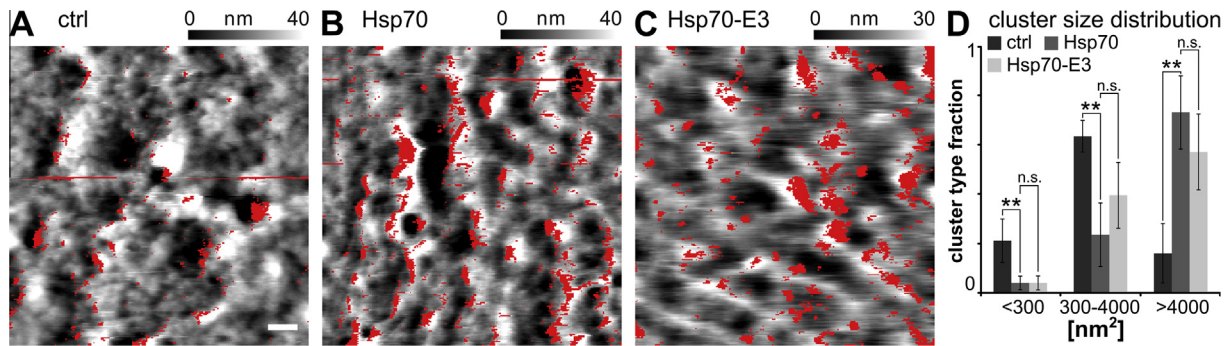


**Fig. 2.** Hsp70 accumulates in enlarged clusters in Hsp70 overexpressing B16 cell membranes. (A)–(C) Nano-organisation of Hsp70 on the cell surface. Control (ctrl), Hsp70 and Hsp70 conjugated to an E3 tag overexpressing cells were fixed and imaged by atomic force microscopy dynamic recognition imaging (TREC). Hsp70 was recognised by cmHsp70.1 antibody or E3-complement peptide K4 linked to the cantilever, respectively (red areas). The topography is displayed in grey, the scale bar is 200 nm. (D) Relative Hsp70 cluster size distribution based on Hsp70 recognition images (one-way ANOVA and subsequent Tukey's test;  $n = 3$ – $4$ ;  $N = 3$ ).

dynamic processes, possibly self-organisation of sHsp70 or interaction with other proteins. As clustering has been shown to facilitate endocytosis of diverse proteins such as LDL-receptors, amyloid precursor protein or  $\beta_1$  integrin in both clathrin-dependent and -independent pathways [14–16], we hypothesized a similar mechanism for sHsp70-mediated endocytosis. To understand whether

Hsp70 clusters exist on the cell surface and whether their size correlates with the effects of Hsp70 overexpression on endocytosis, we studied the nano-organisation of sHsp70 on ctrl, Hsp70 and E3 tagged Hsp70 overexpressing cells [17]. Using an atomic force microscopy cantilever conjugated to anti-Hsp70 antibody or to an E3 interacting K4 peptide, both topography and sHsp70 specific

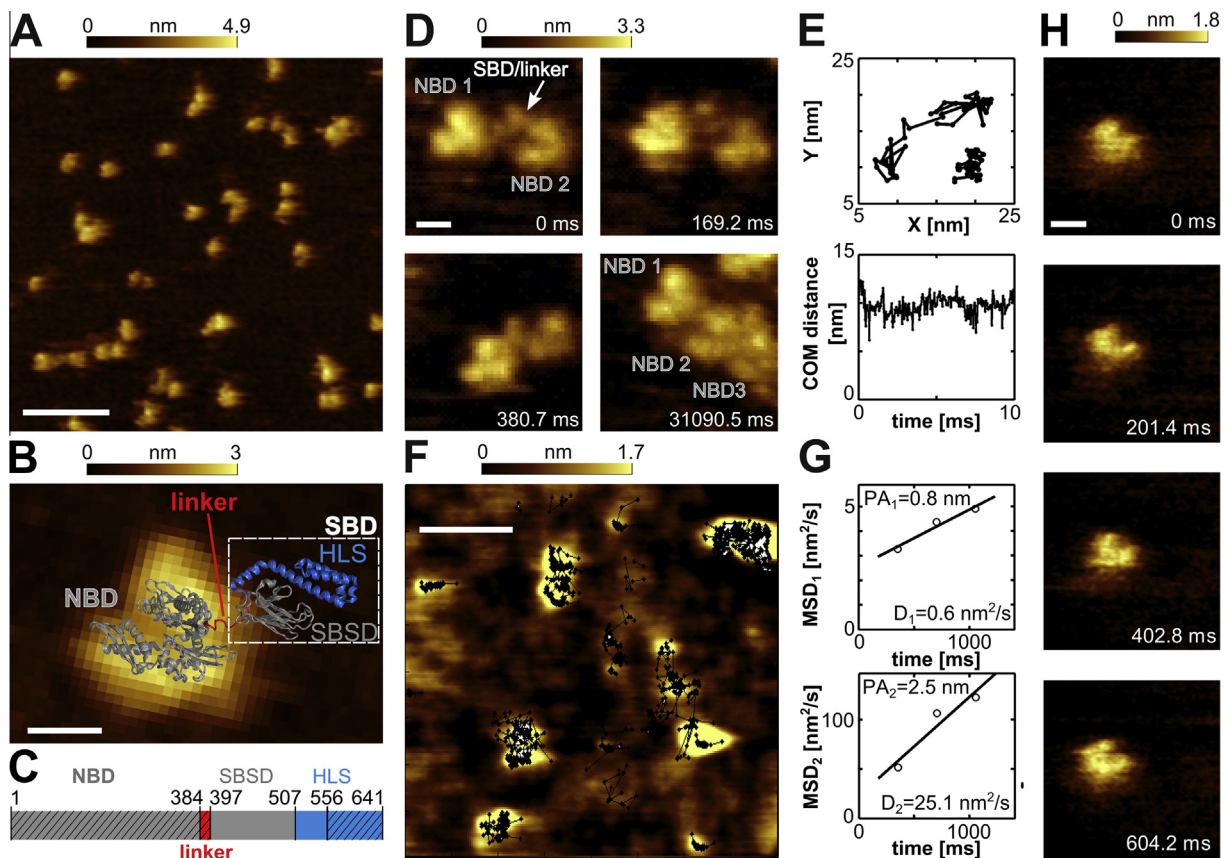


**Fig. 3.** Hsp70 oligomerises on a mica support and clusters on lipid membrane domains *in vitro*. (A) Hsp70 on mica surface visualised by high-speed atomic force microscopy (see Movie E1). Average height of Hsp70 over support was  $3.2 \pm 0.4$  nm ( $n = 112$ ). Scale bar, 200 nm. (B) Superimposition of mica-bound Hsp70 with the crystal structure of the bacterial homologue DnaK (PDB 2KHO) identifies the visualised structure as the N-terminal nucleotide binding domain (NBD). Other structural domains are shown as inter-domain linker (linker) and substrate-binding domain (SBD). SBD consists of the substrate-binding subdomain (SBSD) and the helical lid subdomain (HLS). Scale bar, 4 nm. (C) Schematic representation of the primary structure of human Hsp70. Residues removed in the truncation mutants (Fig. 4) are shaded. (D) High resolution imaging of Hsp70 on mica (see Movie E2) reveals a dynamic nature of Hsp70 dimers as NBD1 moves around NBD2. At 31090.5 ms trimerisation was observed. Scale bar, 5 nm. (E) Trajectories and distances of the centre of mass (COM) of NBD1 and NBD2 derived from Movie E2. (F) High-speed atomic force microscopy imaging of Hsp70 on a model membrane made of PC/SM/cholesterol (see Movie E3). Average height of Hsp70 over the membrane support was  $2.1 \pm 0.7$  nm ( $n = 20$ ). Individual trajectories of Hsp70s are displayed on the average of membrane topography images ( $n = 8$ ) taken from the movie. Scale bar, 100 nm. (G) Analysis of Hsp70 trajectories recorded on the model membrane yielded an immobile ( $47.4 \pm 0.4\%$  of Hsp70 particles, upper panel) and a mobile fraction (lower panel). D is diffusion coefficient, PA is positional accuracy. (H) High-speed atomic force microscopy of Hsp70 on a PC/SM/cholesterol model membrane identifying the NBD as membrane anchoring domain (compare to Fig. 3B). Scale bar, 10 nm.

recognition images were recorded beyond optical resolution limits [18]. The Hsp70-E3/K4 system served as a control for the Hsp70/antibody system. As shown in Fig. 2, recognition maps (displayed in red) revealed that sHsp70 tended to accumulate in nano-domains (or clusters). In agreement with our hypothesis, a remarkable increase in cluster size from small ( $\leq 300$  nm<sup>2</sup>, equivalent circular  $\phi \sim 20$  nm) and medium ( $>300$  nm<sup>2</sup>,  $<4000$  nm<sup>2</sup>) to large clusters ( $\geq 4000$  nm<sup>2</sup>, equivalent circular  $\phi \sim 70$  nm) was observed as a result of Hsp70 overexpression. The larger cluster sizes of sHsp70 were also paralleled with a twofold increase in the surface density of Hsp70 on Hsp70 overexpressing cells compared to control (see Table E1), matching our previous data acquired by flow cytometry [9].

A possible factor that may facilitate clustering of sHsp70 is oligomerisation. In line with previous data obtained with biochemical measurements [10], dimers and higher order oligomers of recombinant human Hsp70 could be visualised by high resolution, high-speed atomic force microscopy at a liquid-solid interface [19]. Remarkably, Hsp70 monomers, dimers and higher oligomers all had a regular height of  $3.2 \pm 0.4$  nm indicating a uniform orientation on the support (Fig. 3A; Movie E1). Analysing the recombinant protein sample at higher resolution, the nucleotide-binding domains (NBDs) of dimers and trimers could be clearly identified. The substrate-binding domains (SBDs) were poorly resolved likely due to their lack of association to the surface and their flexible connection to the NBD via the linker domain (Fig. 3B–D). Analysis of trajectories of NBDs of the same molecule revealed a fairly stable, yet flexible and dynamic dimer structure with an average distance of  $9.7 \pm 0.9$  nm between the NBDs (Fig. 3D and E; see Movie E2). A dynamic formation of trimers was also evident (Fig. 3D).

The partial uptake of sHsp70 via the cholesterol-dependent CIE (Fig. 1B) and the affinity of Hsp70 to specific lipids such as cholesterol [7,20], may further support accumulation and clustering of sHsp70 in cholesterol-enriched lipid rafts. To test this idea, interaction of recombinant Hsp70 with a supported bilayer was monitored by high-speed atomic force microscopy. A segregated lipid layer of PC/SM/cholesterol was used as an artificial model, where lower non-raft and higher raft-like lipid domain areas were apparent [21]. Hsp70 added to the lipid layer essentially localised and clustered on the elevated, raft like domains (Fig. 3F). With nearly equal probability, a practically immobile and a mobile fraction of Hsp70 could be detected in all lipid domains analysed (Fig. 3G, see Movie E3). Notably, the reduced average height of Hsp70 on the lipid bilayer ( $2.1 \pm 0.7$  nm), as compared to impenetrable mica ( $3.2 \pm 0.4$  nm), indicated a partial insertion of Hsp70 into the lipid layer (Fig. 3A and F;  $P < 0.001$ ). Furthermore, time-resolved high-resolution images revealed the NBD as the lipid interaction site (Fig. 3H). This finding was in good agreement with previous reports on a single amino acid mutation in the NBD that impaired Hsp70 membrane interaction [22,23]. Taken together, these data showed that Hsp70 was able to interact with artificial lipid membranes via its NBD domain and accumulated in raft-like lipid domains, where it oligomerised and formed clusters.

Finally, to test if Hsp70 self-organisation stimulates endocytosis, we used fragments of the recombinant human Hsp70 with impaired oligomerisation properties, hence capable of interfering with the oligomerisation of wt full length Hsp70. It has been recently proposed that Hsp70 oligomerisation is mediated by the inter-domain linker (linker), connecting the NBD and the SBD, and the C-terminal part of the helical lid subdomain (HLS) of the

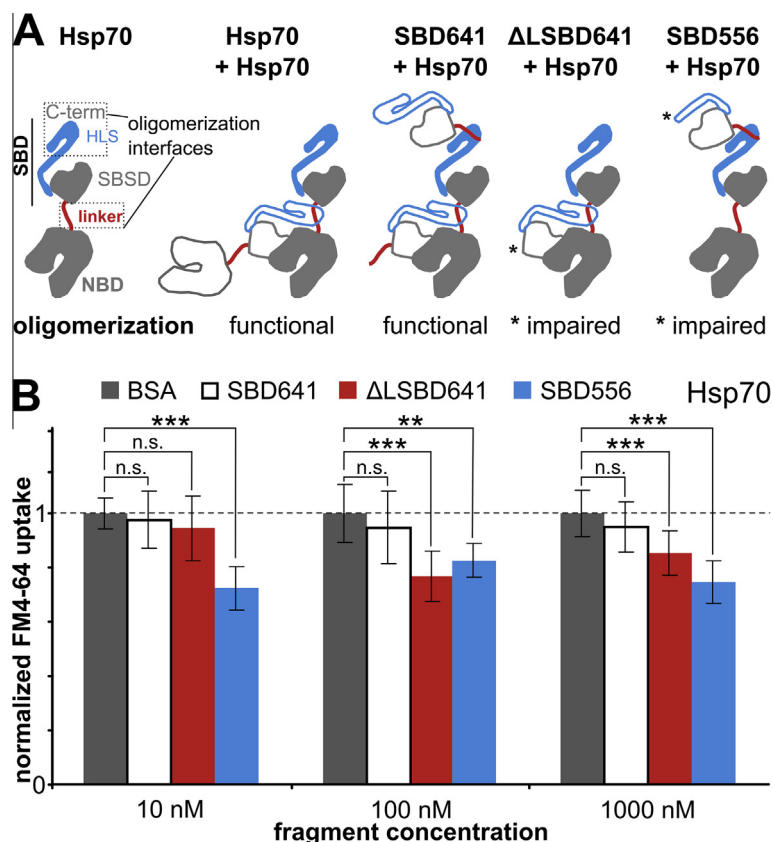


**Fig. 4.** De-oligomerising fragments of recombinant Hsp70 impair endocytosis in B16 cells. (A) Schematic drawing of Hsp70 fragments interacting with the full length protein. (B) FM4-64 uptake in Hsp70 overexpressing cells treated with fragments SBD641,  $\Delta$ LSBD641, SBD556 or BSA at the given concentrations overnight was followed on a plate reader (one-way ANOVA and subsequent Tukey's test; 10 nM  $n = 17$ – $12$ ,  $N = 5$ ; 100 nM  $n = 8$ – $9$ ,  $N = 2$ ; 1000 nM  $n = 17$ – $23$ ,  $N = 5$ ).

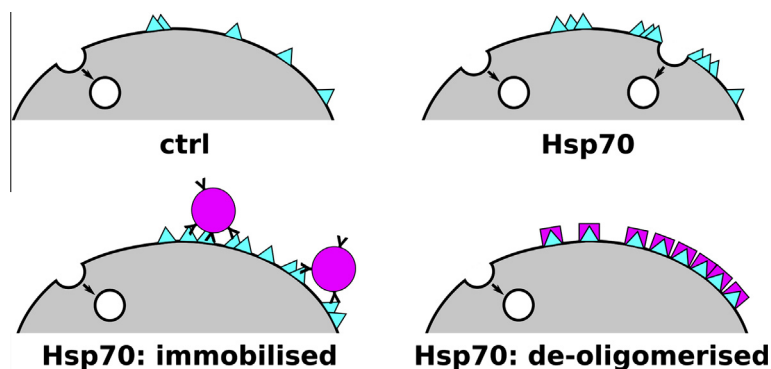


**Fig. 5.** Schematic model for surface localised Hsp70-mediated facilitation of endocytosis in cancer cells. In control cells with low level of Hsp70, tumour cell surface localised Hsp70 (sHsp70) is localised in smaller size clusters on the plasma membrane. Upregulating intracellular Hsp70 expression, as in various forms of cancer [2], is accompanied with an elevated sHsp70 concentration [9]. sHsp70 at higher concentration forms larger clusters on the plasma membrane, which enables facilitation of CIE. Immobilisation or de-oligomerisation of sHsp70 interfere with sHsp70-mediated facilitation of endocytosis, indicating that dynamics of sHsp70 as well as its ability to oligomerise are important to exert an effect on endocytosis.

SBD [10]. By adding SBD fragments of recombinant human Hsp70 lacking either of the two oligomerisation interfaces ( $\Delta$ LSBD641 variant without the linker and SBD556 variant without the C-terminal part of the HLS; see Figs. 3C and 4A) to Hsp70 overexpressing cells, we expected to reduce sHsp70 oligomerisation, hence endocytosis. As these fragments lacked the NBD domain, we thereby eliminated potential binding of the fragments to the cell membrane (Fig. 3H). Indeed, interfering with oligomerisation of sHsp70 by the SBD556 and  $\Delta$ LSBD641 fragments significantly reduced the FM4-64 uptake in a concentration dependent manner (Fig. 4B, up to 27.7% inhibition). In contrast, neither inert BSA nor a control fragment with the two fully functional oligomerising interfaces, did affect endocytosis at any concentration tested. It should be noted that administering with *wt* full length recombinant Hsp70 slightly increased FM4-64 uptake (data not shown). It is also noteworthy that extent of the observed inhibition was comparable to the stimulation of endocytosis by Hsp70 overexpression (Fig. 1A), supporting the idea of an oligomerisation dependent mechanism.

In conclusion, we propose a novel function of the cell surface localised Hsp70 as a stimulator of CIE. Accumulation of overexpressed Hsp70 in large size nano-domains on the cell surface, paralleled with a reversible increase in endocytosis driven by sHsp70 oligomerisation, strongly suggest a clustering dependent mechanism for sHsp70-mediated increase in endocytosis (Fig. 5). Interestingly, oligomerisation was previously described as a requirement for raft-association and transcytosis of GPI-GFP [24,25] as well as for the recognition and internalisation of toxic amylin [26]. Here we first describe sHsp70 as a potential regulator of such oligomerisation and clustering dependent endocytic events. Preferential interaction of Hsp70 with specific lipids, its ability to cluster on cell membranes and its chaperone function support a significant role for sHsp70 in endocytosis. In line with this argument, clustering and interaction of specific surface molecules with lipid rafts are thought to enable formation of membrane curvature and invagination, hence initiating endocytosis even without adaptor proteins at the cytosolic side [27,28]. We suggest that sHsp70, when present in cancer cell membranes, may facilitate the raft associated CIE in an analogous manner. Revealing additional components of the CIE machinery and further understanding of the mechanism of action of known regulators, such as glycosphingolipids, Galectin-3 or sHsp70 will be fostering this emerging field [27].

Altered endocytosis is a typical feature of cancer, where dynamic remodelling and recycling routes at the plasma membrane support tumour cell survival and progression [8]. As Hsp70

is frequently upregulated in tumours, the resulting increased sHsp70 levels [4,9] could stimulate endocytosis for the benefit of the tumour [29,30]. Inhibition of the sHsp70-mediated stimulation of endocytosis, as shown in this study, may therefore represent an adjuvant therapeutic strategy against cancer. At the same time, tumour specific surface localisation of Hsp70 allows specific drug targeting of cancer cells [31,32], where sHsp70-mediated increase in endocytosis would enhance the efficiency of drug treatment. sHsp70-mediated stimulation of endocytosis, reported in this paper, represents a novel cancer specific mechanism and further validates the tumour marker sHsp70 for efficient anti-cancer drug delivery. In future, we aim to follow our current working hypothesis in order to characterise the mechanism of regulation of endocytosis by sHsp70.

### Competing interest

The authors declare no competing interests.

### Acknowledgments

We thank Prof. Hermann J. Gruber (Institute for Biophysics, Johannes Kepler University, Linz, Austria) for developing the atomic force microscopy tip chemistry protocol for the NHS-PEG-maleimide linker. Prof. Boris Margulis (Institute of Cytology, Russian Academy of Sciences, St. Petersburg, Russia) kindly provided us with full length recombinant Hsp70.

This work was funded by the European Regional Development Fund (EFRE), the state of Upper Austria. Laszlo Vigh was supported by the Hungarian Basic Research Fund (OTKA, No. 100857). Nunilo Cremades is a Royal Society Dorothy Hodgkin Research Fellow.

### Appendix A. Supplementary data

Supplementary data associated with this article can be found, in the online version, at <http://dx.doi.org/10.1016/j.febslet.2015.07.037>.

### References

- [1] Mayer, M.P. (2013) Hsp70 chaperone dynamics and molecular mechanism. *Trends Biochem. Sci.* 38, 507–514.
- [2] Calderwood, S.K., Khaleque, M.A., Sawyer, D.B. and Ciocca, D.R. (2006) Heat shock proteins in cancer: chaperones of tumorigenesis. *Trends Biochem. Sci.* 31, 164–172.



- [3] Juhasz, K., Lipp, A.-M., Nimmervoll, B., Sonnleitner, A., Hesse, J., Haselgruebler, T. and Balogi, Z. (2013) The complex function of Hsp70 in metastatic cancer. *Cancers* 6, 42–66.
- [4] Hantschel, M., Pfister, K., Jordan, A., Scholz, R., Andreesen, R., Schmitz, G., Schmetzer, H., Hiddemann, W. and Multhoff, G. (2000) Hsp70 plasma membrane expression on primary tumor biopsy material and bone marrow of leukemic patients. *Cell Stress Chaperones* 5, 438–442.
- [5] Multhoff, G., Botzler, C., Jennen, L., Schmidt, J., Ellwart, J. and Issels, R. (1997) Heat shock protein 72 on tumor cells: a recognition structure for natural killer cells. *J. Immunol.* 158, 4341–4350.
- [6] Stangl, S., Gehrmann, M., Riegger, J., Kuhs, K., Riederer, I., Sievert, W., Hube, K., Mocikat, R., Dressel, R., Kremmer, E., Pockley, A.G., Friedrich, L., Vigh, L., Skerra, A. and Multhoff, G. (2011) Targeting membrane heat-shock protein 70 (Hsp70) on tumors by cmHsp70.1 antibody. *Proc. Natl. Acad. Sci.* 108, 733–738.
- [7] Vega, V.L., Rodriguez-Silva, M., Frey, T., Gehrmann, M., Diaz, J.C., Steinem, C., Multhoff, G., Arispe, N. and De Maio, A. (2008) Hsp70 translocates into the plasma membrane after stress and is released into the extracellular environment in a membrane-associated form that activates macrophages. *J. Immunol.* 180, 4299–4307.
- [8] Mosesson, Y., Mills, G.B. and Yarden, Y. (2008) Derailed endocytosis: an emerging feature of cancer. *Nat. Rev. Cancer* 8, 835–850.
- [9] Juhasz, K., Thuenauer, R., Spachinger, A., Duda, E., Horvath, I., Vigh, L., Sonnleitner, A. and Balogi, Z. (2013) Lysosomal rerouting of Hsp70 trafficking as a potential immune activating tool for targeting melanoma. *Curr. Pharm. Des.* 19, 430.
- [10] Aprile, F.A., Dhulesia, A., Stengel, F., Roodveldt, C., Benesch, J.L.P., Tortora, P., Robinson, C.V., Salvatella, X., Dobson, C.M. and Cremades, N. (2013) Hsp70 Oligomerization Is Mediated by an Interaction between the Interdomain Linker and the Substrate-Binding Domain. *PLoS One* 8, e67961.
- [11] Yamamoto, D., Uchihashi, T., Kadera, N., Yamashita, H., Nishikori, S., Ogura, T., Shibata, M. and Ando, T. (2010) High-speed atomic force microscopy techniques for observing dynamic biomolecular processes. *Methods in Enzymology*, pp. 541–564, Elsevier.
- [12] Sharma, D.K., Choudhury, A., Singh, R.D., Wheatley, C.L., Marks, D.L. and Pagano, R.E. (2003) Glycosphingolipids internalized via caveolar-related endocytosis rapidly merge with the clathrin pathway in early endosomes and form microdomains for recycling. *J. Biol. Chem.* 278, 7564–7572.
- [13] Vega, V.L., Charles, W. and De Maio, A. (2010) A new feature of the stress response: increase in endocytosis mediated by Hsp70. *Cell Stress Chaperones* 15, 517–527.
- [14] Heuser, J.E. and Anderson, R.G. (1989) Hypertonic media inhibit receptor-mediated endocytosis by blocking clathrin-coated pit formation. *J. Cell Biol.* 108, 389–400.
- [15] Sharma, D.K., Brown, J.C., Cheng, Z., Holicky, E.L., Marks, D.L. and Pagano, R.E. (2005) The glycosphingolipid, lactosylceramide, regulates  $\beta$ 1-integrin clustering and endocytosis. *Cancer Res.* 65, 8233–8241.
- [16] Schneider, A., Rajendran, L., Honsho, M., Gralle, M., Donnert, G., Wouters, F., Hell, S.W. and Simons, M. (2008) Flotillin-dependent clustering of the amyloid precursor protein regulates its endocytosis and amyloidogenic processing in neurons. *J. Neurosci.* 28, 2874–2882.
- [17] Yano, Y., Yano, A., Oishi, S., Sugimoto, Y., Tsujimoto, G., Fujii, N. and Matsuzaki, K. (2008) Coiled-coil tag – probe system for quick labeling of membrane receptors in living cell. *ACS Chem. Biol.* 3, 341–345.
- [18] Chitchevlova, L.A., Waschke, J., Wildling, L., Drenckhahn, D. and Hinterdorfer, P. (2007) Nano-scale dynamic recognition imaging on vascular endothelial cells. *Biophys. J.* 93, L11–L13.
- [19] Preiner, J., Kadera, N., Tang, J., Ebner, A., Brameshuber, M., Blaas, D., Gelbmann, N., Gruber, H.J., Ando, T. and Hinterdorfer, P. (2014) IgGs are made for walking on bacterial and viral surfaces. *Nat. Commun.* 5.
- [20] Gehrmann, M., Liebisch, G., Schmitz, G., Anderson, R., Steinem, C., De Maio, A., Pockley, G. and Multhoff, G. (2008) Tumor-specific Hsp70 plasma membrane localization is enabled by the glycosphingolipid Gb3. *PLoS One* 3, e1925.
- [21] Sullan, R.M.A., Li, J.K., Hao, C., Walker, G.C. and Zou, S. (2010) Cholesterol-dependent nanomechanical stability of phase-segregated multicomponent lipid bilayers. *Biophys. J.* 99, 507–516.
- [22] Kirkegaard, T., Roth, A.G., Petersen, N.H.T., Mahalka, A.K., Olsen, O.D., Moilanen, I., Zylicz, A., Knudsen, J., Sandhoff, K., Arenz, C., et al. (2010) Hsp70 stabilizes lysosomes and reverts Niemann-Pick disease-associated lysosomal pathology. *Nature* 463, 549–553.
- [23] Mahalka, A.K., Kirkegaard, T., Jukola, L.T.I., Jäättelä, M. and Kinnunen, P.K.J. (2014) Human heat shock protein 70 (Hsp70) as a peripheral membrane protein. *Biochim. Biophys. Acta* 1, 1–10.
- [24] Brameshuber, M., Weghuber, J., Ruprecht, V., Gombos, I., Horvath, I., Vigh, L., Eckerstorfer, P., Kiss, E., Stockinger, H. and Schütz, G.J. (2010) Imaging of mobile long-lived nanoplateforms in the live cell plasma membrane. *J. Biol. Chem.* 285, 41765–41771.
- [25] Galmes, R., Delaunay, J.-L., Maurice, M. and Ait-Slimane, T. (2013) Oligomerization is required for normal endocytosis/transcytosis of a GPI-anchored protein in polarized hepatic cells. *J. Cell Sci.* 126, 3409–3416.
- [26] Trikha, S. and Jeremic, A.M. (2011) Clustering and internalization of toxic amylin oligomers in pancreatic cells require plasma membrane cholesterol. *J. Biol. Chem.* 286, 36086–36097.
- [27] Lakshminarayan, R., Wunder, C., Becken, U., Howes, M.T., Benzing, C., Arumugam, S., Sales, S., Ariotti, N., Chambon, V., Lamaze, C., Loew, D., Shevchenko, A., Gaus, K., Parton, R.G. and Johannes, L. (2014) Galectin-3 drives glycosphingolipid-dependent biogenesis of clathrin-independent carriers. *Nat. Cell Biol.* 16, 595–606.
- [28] Romer, W., Berland, L., Chambon, V., Gaus, K., Windschiegel, B., Tenza, D., Aly, M.R., Fraissier, V., Florent, J.C., Perrais, D., Lamaze, C., Raposo, G., Steinem, C., Sens, P., Bassereau, P. and Johannes, L. (2007) Shiga toxin induces tubular membrane invaginations for its uptake into cells. *Nature* 450, 670–675.
- [29] Joffre, C., Barrow, R., Ménard, L., Calleja, V., Hart, I.R. and Kermorgant, S. (2011) A direct role for Met endocytosis in tumorigenesis. *Nat. Cell Biol.* 13, 827–837.
- [30] Sigismund, S., Woelk, T., Puri, C., Maspero, E., Tacchetti, C., Transidico, P., Di Fiore, P.P. and Polo, S. (2005) Clathrin-independent endocytosis of ubiquitinated cargos. *Proc. Natl. Acad. Sci. U.S.A.* 102, 2760–2765.
- [31] Gaca, S., Reichert, S., Multhoff, G., Wacker, M., Hehlhans, S., Botzler, C., Gehrmann, M., Rödel, C., Kreuter, J. and Rödel, F. (2013) Targeting by cmHsp70.1-antibody coated and survivin miRNA plasmid loaded nanoparticles to radiosensitize glioblastoma cells. *J. Control. Release Off. J. Control. Release Soc.* 172, 201–206.
- [32] Stangl, S., Gehrmann, M., Dressel, R., Alves, F., Dullin, C., Themelis, G., Ntziachristos, V., Staebelin, E., Walch, A., Winkelman, I. and Multhoff, G. (2011) In vivo imaging of CT26 mouse tumours by using cmHsp70.1 monoclonal antibody. *J. Cell Mol. Med.* 15 (4), 874–887.